A Fully 3-D-Printing-Compatible *E*-Plane Elliptical Waveguide Junction for Power Dividing/Combining Applications

Sicheng Chen[#$*1], Jin Li[#$*2], Tao Yuan[#$*^]
[#]Guangdong Provincial Mobile Terminal Microwave and Millimeter-Wave Antenna Engineering Research Center, College of Electronics and Information Engineering, Shenzhen University, China
[$]Guangdong-Hong Kong Joint Laboratory for Big Data Imaging and Communication, China
[*]State Key Laboratory of Millimeter Waves, China
[^]ATR National Key Laboratory of Defense Technology, College of Electronics and Information Engineering, Shenzhen University, China
[1]chensicheng2018@email.szu.edu.cn, [2]jinli.cie@szu.edu.cn

***Abstract*— In this paper, a new class of 3-D-printing-compatible *E*-plane elliptical waveguide (EWG) junction is proposed for wideband power dividers/combiners. The junction is based on an EWG architecture with tailored power dividing and impedance-matching structures that are configured in a Y-shape profile. The junction is devised according to a specified orientation for 3-D printing and it features smooth and intrinsically self-supportable waveguide sidewalls. Compared to conventional rectangular waveguide junctions, the proposed EWG junction exhibits dramatically enhanced structural compatibility with additive manufacturing technology. A novel four-way EWG-junction-based power divider is demonstrated at *Ka* band. The power divider is prototyped monolithically by incorporating Polyjet 3-D printing and electroless copper plating processes. RF performance of the power divider shows a return loss of mostly over 20 dB, transmission coefficients of averagely −6.5 dB, and small amplitude and phase imbalances across the entire *Ka* band, successfully validating the wideband and low-loss characteristics of the proposed EWG junction.**

***Keywords*— elliptical waveguide, Polyjet, 3-D-printing-compatible, waveguide bend, waveguide junction, waveguide power divider/combiner.**

I. Introduction

Waveguide junctions with power dividing and combining functionalities have been extensively utilized as the enabling circuit element in the feeding network of high-power RF frontends. Conventional rectangular waveguide (RWG) junctions include *E*-plane and *H*-plane architectures with the waveguide arms mainly configured into T-shape and Y-shape profiles. They are capable of achieving a wide operational bandwidth by incorporating a variety of impedance-matching structures such as printed circuit board (PCB) elements [1], metal irises [2], metal posts [3], and ridged and transition waveguide segments [4]–[6]. Conventional RWG junctions are manufactured by employing metal-based computer numerical controlled (CNC) machining process and the junction model needs to be split into several parts to facilitate machining of the impedance-matching structures inside the waveguide pipes. Unfortunately, CNC machining and assembly of geometrically complex waveguide structures are challenging.

An alternative solution to address this challenge is manufacturing the waveguide structure monolithically with the help of 3-D printing technology. Many 3-D printed passive devices containing RWG junctions such as orthomode transducers (OMTs) [7], [8], magic-Ts [9], and power dividers [10], [11] have been demonstrated. The 3-D printed waveguide devices feature reduced redundant structures and enhanced flexibility in the geometrical design. Monolithic prototyping of these devices requires minimized use of internal support that allows correct formation of overhanging structures and suspended ceilings of the waveguide. To fulfill this requirement, the 3-D electronic model is usually preset with an appropriate posture in the 3-D printing platform. The posture determines a vertical orientation for 3-D printing and along this orientation most of the waveguide sidewalls can be formed without using any support. However, manually selecting a posture as such is difficult for complex waveguide geometries. In addition, 3-D printing the waveguide structure in a tilted posture inevitably produces deformation and the deformation would deteriorate RF performance of the device. For example, the measured port and polarization isolations of the 3-D printed OMTs in the work of [7] and [8] are much lower than the simulated values mainly due to the deformed polarization splitters. Similarly,

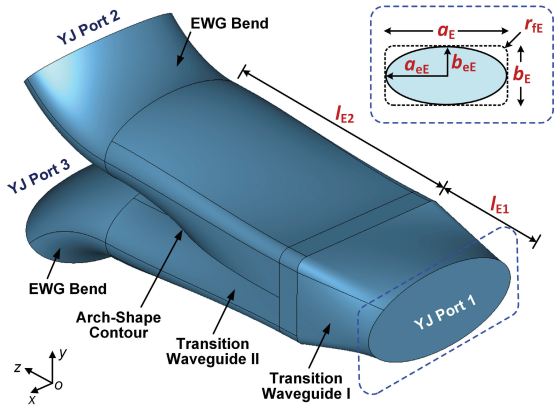

Fig. 1. An air-cavity simulation model of the proposed wideband *E*-plane Y-shape EWG junction. YJ Port 1, YJ Port 2, and YJ Port 3: EWG ports. The blue dashed region illustrates a contour of the EWG port (solid) in comparison with that of the filleted RWG (dash) on the other side of the transition waveguide I.

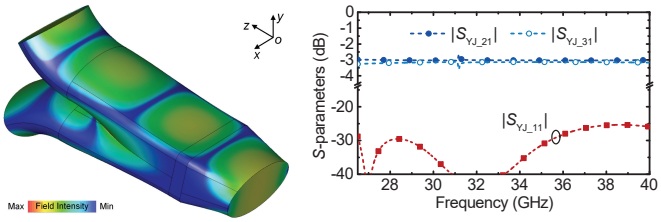

(a) (b)

Fig. 2. EM simulation of the proposed *E*-plane Y-shape EWG junction. (a) The simulated TE_{c11}-mode magnetic field distribution at 31 GHz. (b) The simulated reflection and transmission coefficients. The optimized lengths corresponding to the EM-simulated result are l_{E1} = 4 mm and l_{E2} = 11 mm.

transmission characteristics of the waveguide junctions are impacted by the deformed impedance-matching structures and it is unlikely to compensate the impact through post processing of the 3-D printed parts.

In this work, a geometrical solution compatible with 3-D printing technology is tailored for the waveguide junction to minimize the internal support and the deformation, simultaneously. A new class of *E*-plane elliptical waveguide (EWG) junction is proposed. The junction is devised by incorporating the fundamental principle of additive manufacturing and it is used in the prototype design of a *Ka*-band four-way EWG power divider. The following content of this paper describes design, manufacture, and RF measurement of the power divider.

II. 3-D-Printing-Compatible EWG Power Divider

A. E-Plane Y-Shape Junction

The proposed *E*-plane Y-shape junction is based on an EWG architecture comprising two 45° *E*-plane EWG bends and two transition waveguide segments (I and II) as illustrated in Fig. 1. The input and output EWG ports are defined as YJ Port 1, YJ Port 2, and YJ Port 3 and the EWG supports transmission of the dominant mode TE_{c11}. As the junction is used for power dividing, the TE_{c11} mode is input from the YJ Port 1 and is split into two signal paths propagating to the YJ Port 2 and the YJ Port 3 with an equal amplitude and out of phase. This ideally corresponds to transmission coefficients of $S_{\mathrm{YJ\_21}}$ = $S_{\mathrm{YJ\_31}}$ = $1/\sqrt{2}$ and a reflection coefficient of $S_{\mathrm{YJ\_11}}$ = 0. The transition waveguide I between the EWG port and a filleted RWG segment is built by lofting. The transition waveguide II is composed of two partially nested filleted RWG-to-EWG transitions with the intersecting edge formed naturally into an arch-shape contour. An arch-shaped septum is built as part of the waveguide sidewalls, enabling the power dividing functionality and a "self-supportable" feature of the junction. As can be seen in Fig. 1, the cavity profile is shaped according to a specified orientation, i.e., the oz axis, for 3-D printing and it allows the waveguide sidewalls to be self-supportable as the junction is 3-D printed along this axis. With the specified 3-D printing orientation, slicing for the electronic model of the junction is carried out in the xoy plane and the edge of each sliced layer can be supported by the lower layer without introducing large overhangs. Therefore, the junction can be 3-D printed in this orientation without using any internal support.

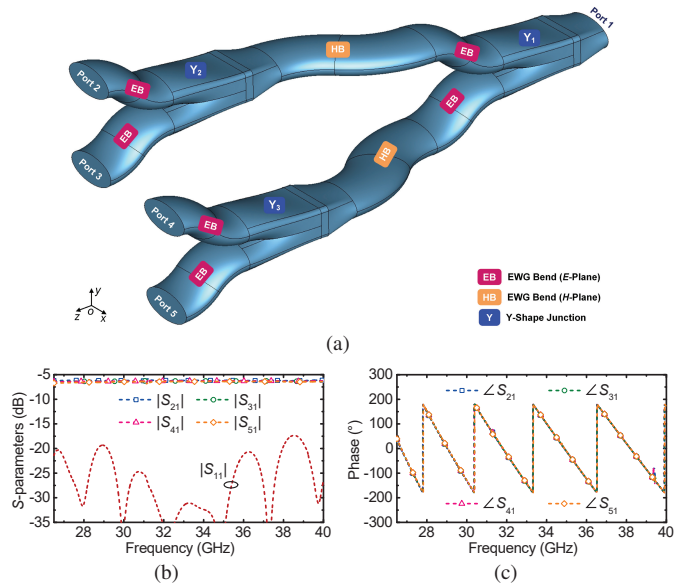

(a) (b) (c)

Fig. 3. Physical modeling and EM simulation of the *Ka*-band four-way EWG power divider. (a) An air-cavity simulation model. (b) The simulated reflection and transmission coefficients. (c) The simulated transmission phase.

It is worth noting that the aforementioned "self-supportable" feature of the junction is tailored for this particular 3-D printing orientation along the oz axis. This means that 3-D printing the junction along other orientations would lose this feature. For example, the support would be used internally for the junction printed along the oy axis. Therefore, the EWG-junction-based waveguide device needs to be shaped along the oz axis as well so that the entire structure of the device can be 3-D printed monolithically with minimized use of support. Fig. 2(a) graphically exemplifies simulated magnetic field distribution of the TE_{c11} mode in the junction. It is interesting to see the similarity in the field distribution of the EWG TE_{c11} mode and the RWG TE_{10} mode. The electromagnetic (EM) simulation is performed in CST Studio Suite [12]. The lengths of semi-major and semi-minor axes of each EWG port, i.e., a_{eE} and b_{eE} as labeled in Fig. 1, are determined to be 3.725 and 1.8 mm, respectively, according to [13] that has evidenced a wideband transmission characteristic of the EWG. The calculated cutoff frequency and bandwidth of the EWG corresponding to this size are 24 and 19.9 GHz, respectively. The bandwidth covers the entire *Ka* band, and therefore, it is reasonable to use the EWG architecture for realization of wideband microwave devices. The cross-sectional size of the filleted RWG is determined to be close to that of the EWG and the related dimensions are a_{E} = 7.45 mm, b_{E} = 3.6 mm, and r_{fE} = 0.5 mm. The position of the EWG bends are adjusted to be tangential with each other and the lengths l_{E1} and l_{E2} of the transition waveguides, as labeled in Fig. 1, are optimized to achieve wideband and low-reflection performance. The simulated *Ka*-band frequency response of the optimized junction geometry is plotted in Fig. 2(b), showing full-band

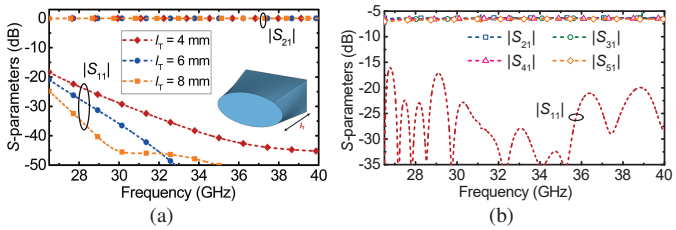

Fig. 4. The simulated reflection and transmission coefficients of the air-cavity models. (a) The EWG-to-RWG transition. (b) The *Ka*-band four-way EWG power divider with the transitions.

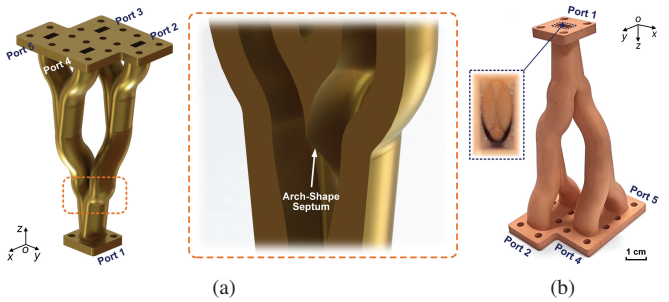

Fig. 5. 3-D illustrations of the *Ka*-band four-way EWG power divider. (a) The package model for 3-D printing. The cutaway view in the dashed region shows the internal profile of the *E*-plane Y-shape EWG junction. (b) Photographs of the manufactured power divider. The inset in the dashed region provides a close-up view of the 3-D printed and copper-plated arch-shape septum.

equal power dividing performance with a reflection coefficient of lower than −25 dB.

B. Four-Way Power Divider

A *Ka*-band four-way EWG power divider is then designed on the basis of the proposed junction and its air-cavity simulation model is illustrated in Fig. 3(a). The power divider is composed of three EWG junctions in connection with two groups of EWG bends. Specifically, the output ports of the first-level EWG junction (Y_1) are connected to the input ports of the secondary two EWG junctions (Y_2 and Y_3) with consecutive *E*-plane and *H*-plane EWG bends (EB and HB). The four output ports of the Y_2 and Y_3 junctions are extended with *E*-plane EWG bends to adapt to waveguide flanges. Combination of the 45° *E*-plane bends and 45° *H*-plane bends produces a streamlined and 3-D-printing-compatible power divider geometry. Figs. 3(b) and 3(c) present the simulated RF performance of the designed four-way EWG power divider. It shows an equal-amplitude and in-phase power dividing characteristic at the Ports 2–5. The EWG bends exhibit low loss and low reflection and would not degrade RF performance of the power divider. The simulated reflection and transmission coefficients of the power divider are mostly lower than −20 dB and (−6.5 ± 0.3) dB, respectively.

All the EWG ports are transitioned to standard WR28 RWG ports to facilitate RF measurement of the power divider and a short segment of EWG-to-RWG transition is used for each port. Fig. 4(a) shows the simulated RF performance of the transition waveguide in different lengths. A transition length l_T of 6 mm is selected to tradeoff the size and reflection. Fig. 4(b) presents the EM-simulated result of the power divider with the transitions and it shows little variation as compared to the one in Fig. 3(b). Fig. 5(a) illustrates the designed *Ka*-band power divider in a monolithic package model, where the four WR28 flanges at the output ports are combined to enhance mechanical strength of the package. As can be seen in Fig. 5(a), intersection of the two EWG bends forms the self-supportable arch-shape septum that can be 3-D printed along the oz axis with minimized risk of collapse.

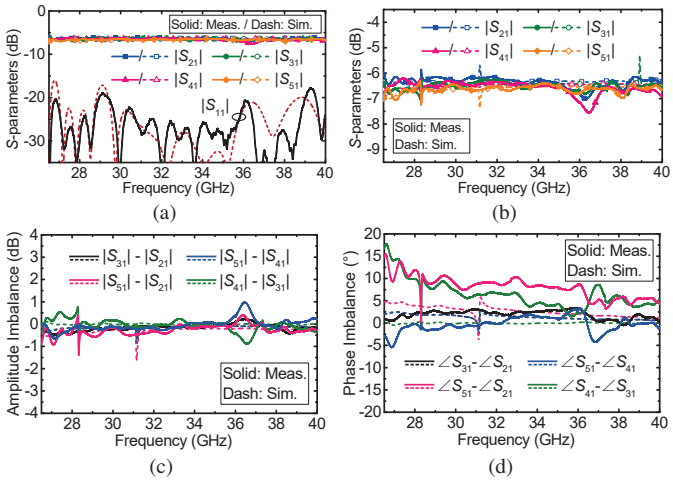

Fig. 6. The EM-simulated and RF-measured results of the four-way EWG power divider. A root-mean-square surface roughness of 2 μm was used for copper (σ = 5.96 × 10^7 S/m) in the simulation. (a) The reflection and transmission coefficients. (b) A zoom-in view of the transmission coefficient. (c) The amplitude imbalance. (d) The phase imbalance.

III. Fabrication, Measurement, and Discussion

The package model of the power divider was prototyped monolithically with a low-density and heat-resistant photosensitive resin by employing high-precision Polyjet 3-D printing process. The 3-D printing was carried out along the $-oz$ axis in a resolution of 20 μm. 3-D printing in this orientation saved most of the external support for the suspended flange without introducing any internal support. The support was 3-D printed with a low-melting-point photosensitive wax and was readily removed by baking and rinsing in the post process of 3-D printing. It should be mentioned that monolithically 3-D printing the model along the $+oz$ axis was still feasible for the utilized Polyjet process and this 3-D printing orientation was also applicable to other techniques such as stereolithography apparatus (SLA) and direct metal laser sintering (DMLS). The 3-D printed resin model was thermally cured, cleaned, and electroless plated with a 5-μm thick layer of copper. Photographs of the manufactured power divider are included in Fig. 5(b).

The power divider was measured by using a Keysight N5224A network analyzer under a two-port waveguide-based through-reflect-line calibration. The RF-measured and EM-simulated results are graphically compared in Fig. 6, showing excellent agreement that successfully validates the wideband and low-loss features of the device. The measured return loss

Table 1. Technical comparison with previously reported waveguide power dividers.

Ref.	f (GHz)	RBW	RL (dB)	No. Ways	WG Archits.	Fabrication Process	M.I.?	AM Comp.
[1]	27–33	20%	>17	2	RWG	CNC+PCB	✗	Poor
[2]	74.9–98.3	[a]27%	[a]>20	4	RWG	N/A	N/A	Poor
[3]	8.2–12.4	40.8%	>16	2	RWG	CNC	✗	Poor
[4]	32–34	6.1%	>15	2	RWG	CNC	✗	Poor
[5]	31–35	12.1%	>25	2	RWG	CNC	✗	Poor
[6]	88.75–97.5	9.47%	>20	3	RWG	CNC	✗	Poor
[10]	8.5–10.5	21%	>14	16	RWG	DMLS	✓	Poor
[11]	10–15	40%	>5	2	RWG	FDM	✓	Poor
T.W.	26.5–40	40.6%	>18	4	EWG	Polyjet	✓	Good

[*]T.W.: This work; RBW: Relative bandwidth; WG Archits.: Waveguide architectures; M.I.: Monolithic integration; AM Comp.: Structural compatibility with additive manufacturing; FDM: Fused deposition modeling.
[a]The simulated values.

(RL) at the Port 1 is over 20 dB at most of *Ka*-band frequencies. The measured transmission coefficients are in a range of (-6.5 ± 0.6) dB. The corresponding amplitude and phase imbalances are in ranges of ± 1 dB and $-5°$–$17.7°$, respectively. The measured amplitude imbalance is consistent with the simulated one except for small fluctuations. The measured phase imbalances $(\angle S_{51} - \angle S_{21})$ and $(\angle S_{41} - \angle S_{31})$ are slightly larger than the simulated ones mainly due to fabrication tolerance and the phase discrepancy indicates intrinsic asymmetry of the Y-shape junction geometry. Major technical attributes of the power divider are summarized in Table 1 in a quantitative comparison with other related demonstrations. The power divider of this work is unique in an EWG architecture that has been rarely used in previous works, because it is rather difficult to manufacture enclosed EWG cavities using CNC machining. The EWG architecture exhibits enhanced compatibility with 3-D printing process without compromising any attractive attribute of the device. The proposed power divider is comparable to those in [1]–[6] in terms of RF performance, and is superior in the monolithic integration with fewer redundant structures. Compared to the work in [10] and [11] , the presented design method is advanced in the shaping along a designated 3-D printing orientation. The method simplifies selection of the 3-D printing orientations for complex waveguide geometries and intrinsically improves the quality of 3-D printed parts.

IV. Conclusion

A geometrically shaped *E*-plane EWG junction has been proposed and a monolithically integrated four-way EWG power divider has been demonstrated at *Ka* band with compact size, good RF performance, and significantly enhanced structural compatibility with 3-D printing technology. The work has validated high reliability of the utilized Polyjet and metal plating processes. The EWG architecture and the method of shaping can be applied to the design of other microwave passive devices.

Acknowledgment

This work was supported in part by the National Key Research and Development Program, China, under Subject No.2021YFA0715301, in part by the State Key Laboratory of Millimeter Waves, China, under Grant No.K202301, in part by the Guangdong Provincial Department of Science and Technology, China, under Project No.2020B1212030002, in part by the Shenzhen Science and Technology Innovation Commission, China, under Project No.KQTD20180412181337494 and Construction and Operation Project of Guangdong Provincial Key Laboratory and Guangdong-Hong Kong-Macau Joint Laboratory, and in part by the Postgraduate Education Branch of the China Education Society of Electronics.

References

[1] Z. Xu, J. Xu, Y. Cui, and C. Qian, "A novel rectangular waveguide T-junction for power combining application," *IEEE Microw. Compon. Lett.*, vol. 25, no. 8, pp. 529–531, Aug. 2015.

[2] S. Hu, K. Song, F. Zhang, Y. Zhu, and Y. Fan, "A novel compact wideband four-way W-band waveguide power divider with low insertion loss," in *Proc. IEEE MTT-S Int. Microw. Workshop Ser. Adv. Mater. Processes RF Terahertz Appl.*, Chengdu, China, Jul. 2016, pp. 1–3.

[3] A. R. Akbarzadeh and Z. Shen, "Waveguide power dividers using multiple posts," *Microw. Opt. Technol. Lett.*, vol. 50, no. 4, pp. 981–984, Apr. 2008.

[4] Y.-S. Liu, D.-C. Niu, and E. S. Li, "Three-port *E*-plane bifurcated waveguide power divider at millimeter-wave frequencies," in *Proc. Asia Pacific Microw. Conf.*, Kaohsiung, Taiwan, Dec. 2012, pp. 998–1000.

[5] J. Ding, Q. Wang, Y. Zhang, and C. Wang, "A novel five-port waveguide power divider," *IEEE Microw. Compon. Lett.*, vol. 24, no. 4, pp. 224–226, Apr. 2014.

[6] G. A. Kumar, B. Biswas, and D. R. Poddar, "A compact broadband riblet-type three-way power divider in rectangular waveguide," *IEEE Microw. Compon. Lett.*, vol. 27, no. 2, pp. 141–143, Feb. 2017.

[7] J. Shen and D. S. Ricketts, "Compact W-band "swan neck" turnstile junction orthomode transducer implemented by 3-D printing," *IEEE Trans. Microw. Theory Techn.*, vol. 68, no. 8, pp. 3408–3417, Aug. 2020.

[8] S. Chen, J. Li, Z. Xu, and T. Yuan, "A *Ka*-band wideband monolithically metallic 3-D printed turnstile junction orthomode transducer with shaped internal profile," in *IEEE MTT-S Int. Microw. Symp. Dig.*, Denver, CO, USA, Jun. 2022, pp. 676–679.

[9] C. Guo, J. Li, Y. Yu, F. Zhang, Y. Zhu, Q. Yang, W. Zhu, S. Zhu, X. Shang, Y. Gao, Y. Wang, G.-L. Huang, Q. S. Cheng, and A. Zhang, "A 3-D printed *E*-plane waveguide magic-T using air-filled coax-to-waveguide transitions," *IEEE Trans. Microw. Theory Techn.*, vol. 67, no. 12, pp. 4984–4994, Dec. 2019.

[10] G.-L. Huang, C.-Z. Han, W. Xu, T. Yuan, and X. Zhang, "A compact 16-way high-power combiner implemented via 3-D metal printing technique for advanced radio-frequency electronics system applications," *IEEE Trans. Ind. Electron.*, vol. 66, no. 6, pp. 4767–4776, Jun. 2019.

[11] A. Genc, T. Goksu, and S. Helhel, "Fabrication of three-dimensional printed rectangular waveguide T-junction with in-phase and equal power division," *Microw. Opt. Technol. Lett.*, vol. 60, no. 8, pp. 2043–2048, Jun. 2018.

[12] (May 2021). CST Studio Suite. Dassault Systémes S.A. [Online]. Available: https://www.3ds.com.

[13] J. G. Kretzschmar, "Wave propagation in hollow conducting elliptical waveguides," *IEEE Trans. Microw. Theory Techn.*, vol. MTT-18, no. 9, pp. 547–554, Sept. 1970.